ACS Macro Letters

Letter

pubs.acs.org/macroletters

Topology-Controlled Relaxation Dynamics of Single Branched Polymers

Danielle J. Mai,[†] Amanda B. Marciel,[‡] Charles E. Sing,[†] and Charles M. Schroeder*[,†,‡,§]

[†]Department of Chemical and Biomolecular Engineering, [‡]Center for Biophysics and Quantitative Biology, and [§]Department of Materials Science and Engineering, University of Illinois at Urbana−Champaign, Urbana, Illinois 61801, United States

Supporting Information

ABSTRACT: In this work, we report the synthesis and direct observation of branched DNA polymers using single molecule techniques. Polymer topology plays a major role in determining the properties of advanced materials, yet understanding the dynamics of these complex macromolecules has been challenging. Here, we study the conformational relaxation dynamics of single surface-tethered comb polymers from high stretch in a microfluidic device. Our results show that the molecular topology of individual branched polymers plays a direct role on the relaxation dynamics of polymers with complex architectures. Macromolecular DNA combs are first synthesized using a hybrid enzymatic-synthetic approach, wherein chemically modified DNA branches and DNA backbones are generated in separate polymerase chain reactions, followed by a "graft-onto" reaction via strain-promoted [3 + 2] azide−alkyne cycloaddition. This method allows for the synthesis of branched polymers with nearly monodisperse backbone and branch molecular weights. Single molecule fluorescence microscopy is then used to directly visualize branched polymers, such that the backbone and side branches can be tracked independently using single- or dual-color fluorescence labeling. Using this approach, we characterize the molecular properties of branched polymers, including apparent contour length and branch grafting distributions. Finally, we study the relaxation dynamics of single comb polymers from high stretch following the cessation of fluid flow, and we find that polymer relaxation depends on branch grafting density and position of branch point along the main chain backbone. Overall, this work effectively extends single polymer dynamics to branched polymers, which allows for dynamic, molecular-scale observation of polymers with complex topologies.

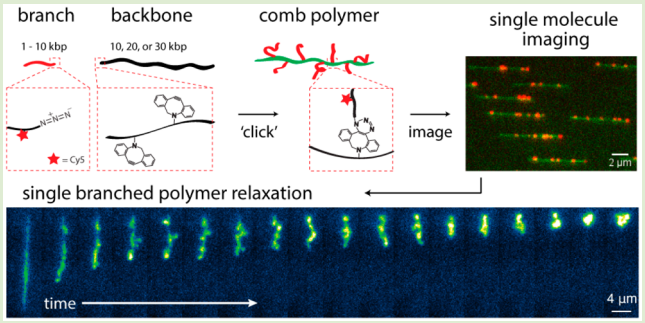

The molecular topology of long chain polymers has long been known to influence the bulk properties of these materials.[1−3] Synthetic polymers used in commercial applications display exceedingly complex topologies, including high grafting densities of side chains, hierarchical branching, and dangling ends.[4,5] In recent years, architecturally complex polymers with well-defined structures such as multiarm stars,[6] H-polymers,[7] and comb polymers[8] have been used as model systems to study the role of molecular topology on nonequilibrium flow dynamics. Recent studies have focused on the impact of macromolecular branching on the emergent, bulk-scale rheological properties of polymer solutions and melts.[7,9] Chain branching results in complex flow properties that differ substantially from linear polymers under similar conditions, such as strain hardening in uniaxial extensional flow under relatively low strain rates.[8] Given the importance of polymeric materials in modern society, it is critical to achieve a molecular-level understanding of polymer dynamics in the context of nonlinear chain topologies.[1−3]

Comb polymers are an architectural subset of branched polymers consisting of side chain branches grafted to a main chain backbone.[1] Comb polymers are a particularly relevant chain architecture occurring in applications such as pharmacokinetics,[10,11] alternative energy solutions,[12] and antifouling surface coatings.[13] The linear and nonlinear viscoelastic properties of comb polymers have been investigated using a combination of approaches including theory, simulations, and bulk rheological experiments.[2,14−17] Recent studies of comb polymer melts have uncovered a hierarchical stress relaxation mechanism that arises due to branched molecular architectures.[17] However, structural heterogeneity within a branched polymer sample has been shown to blur the macroscopic rheological response of branched polymer melts.[7,18] Bulk-level experiments intrinsically average across all molecules and polymer topologies within a sample, which presents a major challenge for studying molecular-based mechanisms such as hierarchical stress relaxation. Moreover, it has been challenging to describe the nonlinear rheological behavior of branched polymers using a universal constitutive model. Theoretical approaches have been used to develop constitutive stress−strain relations for linear[19] and pom-pom[20] polymers, however,

Received: February 21, 2015
Accepted: March 31, 2015
Published: April 2, 2015

DOI: 10.1021/acsmacrolett.5b00140
ACS Macro Lett. 2015, 4, 446−452

Scheme 1. Synthesis of DNA Comb Polymers[a]

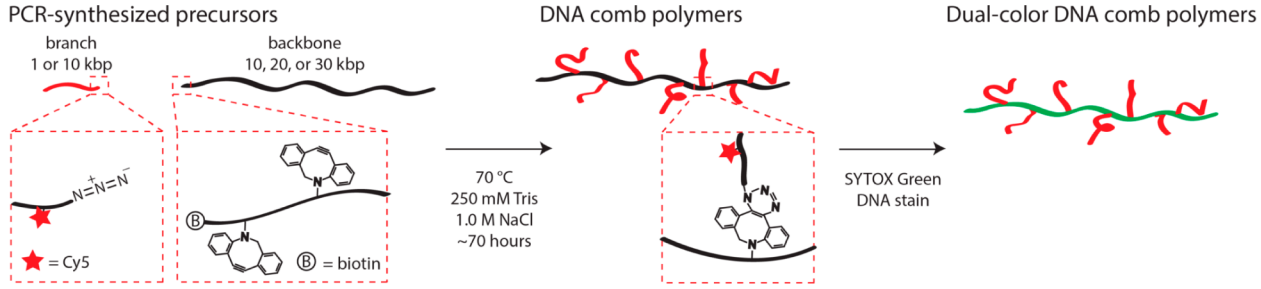

[a]In some cases, dual-color branched polymers are synthesized by direct incorporation of Cy5 dyes into side branches, followed by labeling with an intercalating DNA dye such as SYTOX Green.

the molecular details of polymer topology clearly play a key role in the emergent stress response under flow. Recently, a constitutive model has been developed for comb polymers by extending the pom-pom model to comb-shaped topologies.[21]

In this work, we directly observe the dynamics of branched polymers using single molecule techniques. In particular, we focus on the synthesis and study of comb polymers based on DNA, though by changing the branching distribution, we also observe three-arm stars and H-polymers. For over a decade, DNA has been used as a model system to study the dynamics of single polymer molecules in flow.[22−26] Using this approach, researchers have directly observed intriguing phenomena such as molecular individualism[27] and conformational hysteresis in flow.[28] The vast majority of single molecule DNA studies has focused on linear chain architectures,[25] however, macromolecular DNA stars and pom-poms have been generated via base pairing and hybridization of oligonucleotides at a branched junction. In prior work, Archer and co-workers observed the dynamics of DNA-based star polymers in agarose gels under electric fields.[29,30]

Here, we synthesize branched DNA for single polymer dynamics using a hybrid enzymatic-synthetic approach. The synthesis method is based on a two-step process wherein template-directed synthesis is used to generate polymer backbones with bio-orthogonal reactive groups, followed by a "graft-onto" approach for covalently linking side branches to the main chain backbone (Scheme 1). First, polymerase chain reaction (PCR) is used to enzymatically amplify target sequences from λ-phage DNA in the presence of chemically modified deoxyribonucleotides (dNTPs) and primers. In one reaction, DNA backbones (10, 20, or 30 kbp) are synthesized with internal dibenzylcyclooctyne (DBCO) groups and a terminal biotin tag. In a separate reaction, azide-terminated DNA branches (951 bp or 10 kbp) are synthesized using a chemically modified PCR primer to append an azide group to one branch terminus. In some cases, internal Cy5 dyes are directly incorporated into the low molecular weight branches (951 bp) using modified Cy5-dTTP nucleotides. Following PCR amplification and purification of precursor molecules, branch molecules are chemically grafted onto DNA backbones via strain-promoted [3 + 2] azide−alkyne cycloaddition (SPAAC), thereby generating branched DNA macromolecules suitable for single molecule fluorescence microscopy (SMFM). Bulk absorbance measurements are used to quantify the Cy5 dye loading along DNA branches, revealing an average of 7−8 Cy5 dyes per branch for these reaction conditions. During all preparation and handling steps, care is taken to minimize shearing or degradation of macromolecular structures (for detailed experimental procedures, see Supporting Information, Tables S1−S5 and Figures S1 and S2).

The hybrid enzymatic-synthetic approach allows for precise control over backbone and branch molecular weights. Moreover, branch grafting density can be controlled in an average sense by tuning the relative stoichiometry of side branches during the "graft-onto" reaction. Branch grafting densities and distributions are directly characterized using SMFM, which reveals polymer topologies including three-arm stars (1 branch), H-polymers (2 branches), and comb polymers (>2 branches). Branched DNA polymers are labeled with fluorescent nucleic acid dyes such as SYBR Gold or SYTOX Green, thereby yielding either single-color polymers or dual-color DNA polymers in cases where branches are covalently labeled with Cy5 dye (red) and backbones are labeled with an intercalating dye (green). This approach allows for simultaneous visualization of branch and backbone dynamics using SMFM.

Following synthesis, branched DNA polymers are first characterized using agarose gel electrophoresis (Figure 1). The agarose gel in Figure 1 shows both control and SPAAC reaction products based on a 10 kbp DNA backbone and Cy5-labeled 1 kbp DNA branches. In all cases, negative controls show that DNA backbones without chemically modified DBCO-dNTPs do not react with azide-terminated DNA branches (Lane 2). However, branched polymers are formed by reacting DNA backbones with DBCO modifications (10% of dTTP replaced with 5-DBCO-dUTP) with azide-terminated DNA branches, which generally shows a noticeable shift in agarose gels (Lane 3). In these experiments, negative control and SPAAC reaction samples were both mixed with a ~20 molar excess of azide-terminated, Cy5-labeled branches (red emission). Reactions are carried out in 250 mM Tris buffer (pH 8.0) and 1.0 M NaCl at 70 °C over the course of ~18−70 h, though significant conversion was observed after only a few hours (Supporting Information, Figure S1).

Migration patterns in gel electrophoresis are indicative of polymer chain branching. The negative control sample shown in Figure 1 exhibits green fluorescence emission (only) from the high molecular weight band at 10 kbp, which indicates the absence of Cy5-labeled branch molecules comigrating with natural DNA backbones. However, the presence of DNA comb polymers is indicated in Lane 3 by the comigration of red and green fluorescence emission from the high molecular weight band corresponding to comb polymer. Moreover, the band corresponding to the molecular weight of the DNA backbone is absent in Lane 3, suggesting a near quantitative conversion to branched DNA polymers. Importantly, gel electrophoresis also

DOI: 10.1021/acsmacrolett.5b00140
ACS Macro Lett. 2015, 4, 446−452

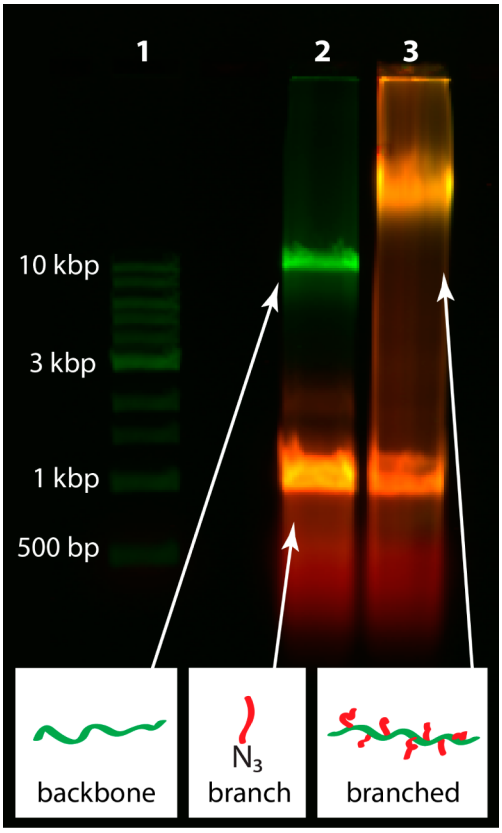

Figure 1. Agarose gel electrophoresis of DNA comb polymers formed by SPAAC. Lane 1: 1 kbp DNA ladder (New England Biolabs). Lane 2: negative control reaction of Cy5-labeled, azide-terminated branches (951 bp) and natural backbones (10 kbp). Lane 3: formation of dual-color branched DNA polymers (>10 kbp) via grafting Cy5-labeled, azide-terminated branches onto DBCO-modified backbones. Gels are stained with SYBR Gold (Invitrogen) and electrophoresed in 1.0% agarose in 1× TAE buffer for 30 min at 120 V.

shows a clear shift in the mobility of branched DNA compared to linear DNA. A decrease in electrophoretic mobility of comb polymers is consistent with previous reports of decreased mobility in DNA with branched architectures, such as stars,[30] pom-poms,[29] and partial denaturation events.[31] This phenomenon is attributed to an increase in molecular weight of DNA combs and the generation of branch sites, which are known to impede the migration of polymers through gel networks due to chain stretch in the transverse direction of the electric field. This topologically driven motion prevents backbone reptation through matrix pores, entangles molecules in the gel network, and transiently traps branch junctions in the matrix, altogether resulting in a significantly reduced electrophoretic mobility for branched DNA molecules.[29−31]

Following gel-based characterization, we used SMFM to directly observe the dynamics of branched polymers with different architectures and contour lengths. In these experiments, polymer molecules are specifically linked to a passivated surface by tethering one terminus of the polymer backbone to a functionalized glass coverslip coated with a mixture of polyethylene glycol (PEG) and PEG-biotin (Figure 2a).[32] PEG-biotin coverslips are first incubated with NeutrAvidin, copiously rinsed with water, and then used to construct a custom microfluidic flow cell by affixing together with a quartz microscope slide. Buffer exchange into the flow cell is achieved using polyethylene tubing epoxied into inlet/outlet ports drilled through the quartz slide. To facilitate specific tethering to the glass coverslip surface, linear and branched DNA are labeled with a biotin moiety at one terminus of the backbone chain. Branched DNA polymers are incubated in the flow cell at a concentration of 10−40 pM, thereby generating a uniform field of single polymers via specific surface tethering. Polymer chains are stretched in pressure-driven flow using a viscous buffer (62.5 or 65% sucrose, yielding 70 or 130 cP solution viscosity, respectively) containing the nucleic acid stain SYTOX Green.

A composite image of dual-color DNA combs stretched under fluid flow is shown in Figure 2b. Comb polymers are clearly indicated by the presence of Cy5-labeled side branches (red) colocalized along DNA backbones (green). Composite dual-color images can be deconstructed to identify SYTOX Green-stained backbones (488/503 nm, excitation/emission peaks) and Cy5-labeled branches (638/670 nm, excitation/emission peaks). Using this approach, we measured the molecular properties of DNA comb polymers, including the distributions of grafted branches (Figure 2c) and flow-stretched end-to-end distances of DNA backbones (Figure 2d). Branch distributions were quantified based on the extended conformations of molecules under fluid flow, such that each diffraction-limited fluorescent "spot" was counted as a branch (Supporting Information, Figure S4). A small fraction (<25%) of the branched polymers excluded from these data showed apparent end-to-end distances <70% of the expected contour length ($L_{stained} \approx 4.3$ or 8.6 μm for 10 or 20 kbp backbones, respectively), which can be attributed to photocleavage during laser excitation or shearing of molecules during handling.

The average backbone end-to-end distance for branched polymers in flow is shown in Figure 2d, where dotted lines indicate the expected extension of molecules in strong flows ($x/L \approx 0.8$ for $100 < Wi < 300$, where Wi is the Weissenberg number).[33] Interestingly, the average end-to-end backbone distance is fairly constant for polymers with identical backbone lengths but variable branch grafting densities in strong shear flow. A complete set of stretched backbone lengths and branch frequency distributions for all samples is provided in Supporting Information (Figures S3 and S5).

Table 1 contains a summary of the molecular properties for branched DNA samples in this work. SMFM allows for direct characterization of the molecular topology of branched DNA molecules over a wide range of conditions. In regards to branching distributions, our single molecule data show that the average number of branches added per backbone is generally less than expected, assuming stoichiometric incorporation of chemically modified DBCO-dUTP and addition of side branches during the "graft-onto" reactions. In particular, we observe an average branch addition of <10 in all cases; however, the theoretical maximum incorporation of DBCO-dUTP in samples 10 A−C, 10 D, and 20 A−D is 500, 1200, and 100, respectively. We hypothesize that the main source of this disparity lies in the discrimination of non-natural, chemically modified nucleotides against natural nucleotides during PCR of DNA backbones. Natural DNA polymerases exhibit an extremely high fidelity for natural nucleotides, and chemical modifications in non-natural bases are known to frustrate DNA polymerases during primer extension synthesis or in moving past a modified template region.[34,35] Evolved DNA polymerases can be used to preferentially incorporate non-natural bases,[36] however, such polymerases could be sensitive to the site of chemical modification on nucleotides and are generally less suitable for long-range PCR used in this work.

DOI: 10.1021/acsmacrolett.5b00140
ACS Macro Lett. 2015, 4, 446−452

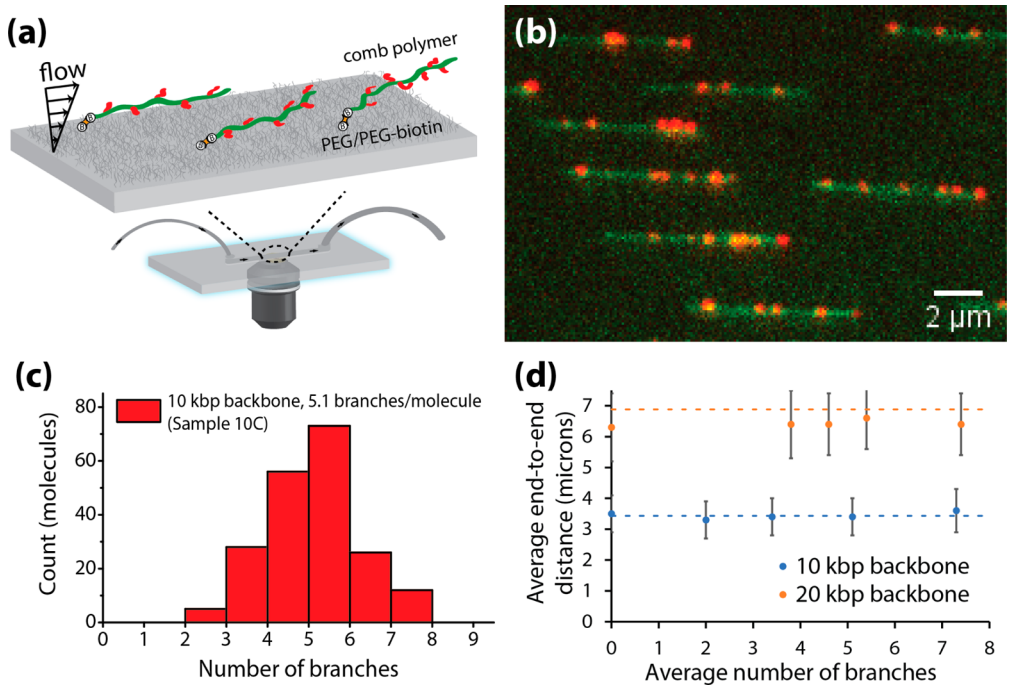

Figure 2. Characterization of branched DNA polymers using single molecule imaging. (a) Schematic of experimental setup showing surface chemistry and custom-built microfluidic flow cell. Glass coverslips are functionalized with a mixture of PEG/PEG-biotin and NeutrAvidin prior to tethering linear or branched DNA via a terminal biotin moiety. (b) Single molecule image of dual-color DNA comb polymers tethered to a surface and stretched under shear flow. Composite image generated by colocalization of SYTOX Green-stained backbones and branches (green) and Cy5-labeled branches (red). (c) Branch frequency distribution for a dual-colored DNA comb sample (10 kbp backbone with ~5.1 branches per molecule, Sample 10 C from Table 1). (d) Average backbone end-to-end distances for DNA comb polymers stretched under fluid flow; error bars reflect standard deviation. Dotted lines indicate the expected extension of linear DNA molecules stretched under tethered shear flow with a flow strength of $100 < Wi < 300$.[33]

Table 1. Molecular Properties of DNA Comb Polymers

sample	backbone length (kbp)	branch length (bp)	substitution of dTTP[a] (%)	molar excess of branches[b]	no. of branches[c]
10 linear	10		0	0	
10 A	10	951	10	5	2.0 ± 1.3
10 B	10	951	10	10	3.4 ± 1.3
10 C	10	951	10	20	5.1 ± 1.0
10 D	10	951	25	50	7.3 ± 1.2
20 linear	20		0	0	
20 A	20	951	1.0	10	3.8 ± 1.7
20 B	20	951	1.0	20	4.6 ± 1.5
20 C	20	951	1.0	50	5.4 ± 1.6
20 D	20	951	1.0	100	7.4 ± 1.7
30 linear	30		0	0	
30 branched	30	10052	1.0	15	1.5 ± 0.7

[a]Percentage of dTTP nucleotide replaced by 5-dUTP-DBCO during PCR to generate DNA backbones. [b]Molar excess of branch molecules in comparison to backbone molecules in SPAAC graft-onto reactions. [c]Mean ± standard deviation. These measurements exclude molecules of stretched end-to-end distances less than 3 or 6 μm for 10 or 20 kbp backbones, respectively. For all samples, the measurements are based on averages over $N > 100$ molecules, except for the 30 kbp branched sample ($N = 45$).

In general, we observe decreased PCR product yields upon substitution of chemically modified nucleotides, which can be overcome by modifying reaction conditions (Supporting Information, Table S4). Incorporation of chemically modified DBCO-dUTP especially hinders efficient replication of higher molecular weight amplicons; for example, in long-range PCR synthesis of 20 and 30 kbp backbones, only 1% substitution of natural dTTP with 5-DBCO-dUTP is tolerated in the reaction under these conditions. In addition to PCR inefficiencies using non-natural bases, it is possible that steric hindrance and electrostatic repulsion results in decreased grafting densities, in particular, linking negatively charged DNA branches onto DNA backbones during SPAAC reactions.

In a second set of experiments, we used SMFM to directly observe the conformational relaxation dynamics of surface-tethered branched polymers (Figure 3). Here, we monitor the relaxation of branched polymers from high stretch (>80% contour length) following cessation of flow, and we report the impact of branch number and position on the relaxation of branched polymers. In this particular experiment, we focus on branched polymers with 30 kbp backbones and 10 kbp branches using single-color fluorescence. The dimensions of

DOI: 10.1021/acsmacrolett.5b00140
ACS Macro Lett. 2015, 4, 446−452

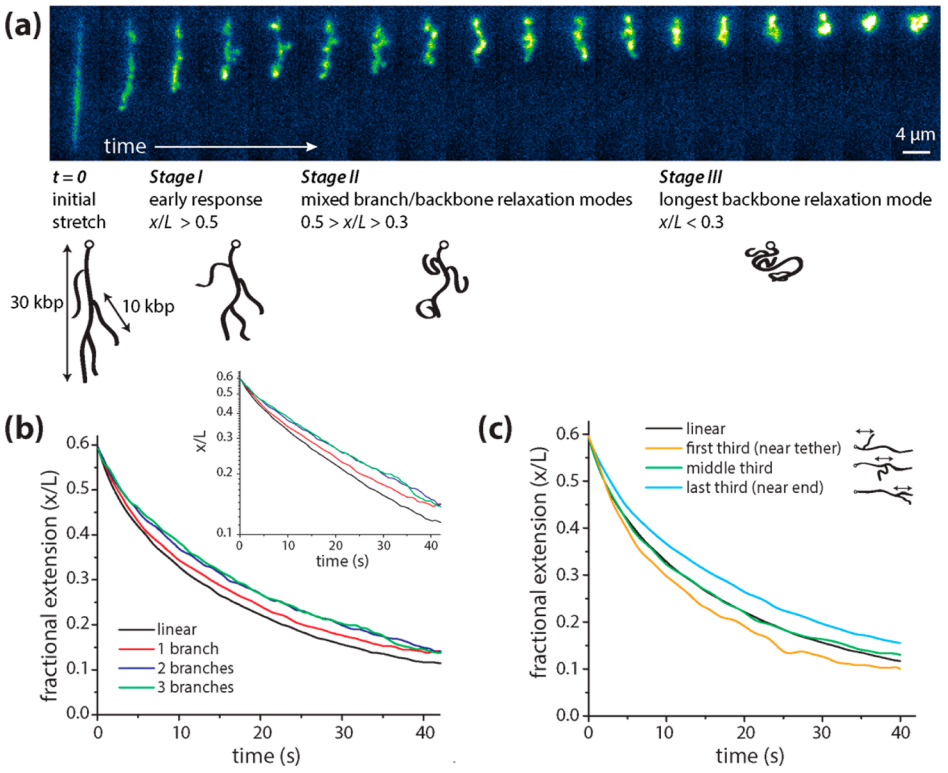

Figure 3. Relaxation dynamics of surface-tethered branched polymer molecules (solvent viscosity $\eta \approx 125$ cP). (a) Time lapse images showing relaxation of a 30 kbp comb polymer with 10 kbp branches after the cessation of shear flow, with corresponding schematic of relaxation mechanisms. Images taken 2.5 s apart. (b) Ensemble-averaged relaxation trajectories for molecules with varying degrees of branching (inset: semilog representation of fractional extension). (c) Ensemble-averaged relaxation trajectories for molecules with a single branch, where the branch position varies along a main chain.

these polymers permit visual counting of side branches as the molecules explore conformational space during relaxation processes. Importantly, these experiments highlight the ability to independently characterize branch and backbone behavior during a dynamic process for branched polymers.

A series of time-lapse images showing the relaxation process for a single surface-tethered branched polymer is shown in Figure 3a. In addition, we provide a schematic illustrating the characteristic branched polymer conformations observed during this process and corresponding stages of relaxation based on quantitative visual analysis of molecular end-to-end distance (x). We note that the schematic and stages are specific to the molecular dimensions observed in this study, and that changes in branch and/or backbone dimensions would subsequently change the observed relaxation processes.

Prior to cessation of shear flow ($t = 0$), polymer molecules exist in a highly extended conformation. At short times following the cessation of flow (*Stage I*), both the backbone and the branches exhibit a simultaneous and rapid entropic response characterized by a sharp decrease in extension with respect to time. At intermediate times in the relaxation process (*Stage II*), we observe mixed modes including branch and backbone relaxation dynamics, such that branches explore various conformational "breathing modes" while the backbone relaxes. We expect mixing of relaxation modes for these molecular topologies, in which branches and backbones are similar in size. At longer times (*Stage III*), the longest mode of relaxation dominates, which corresponds to relaxation of the main chain backbone for this specific molecular architecture, and polymer molecules ultimately appear as fluctuating random coils with nonlinear topologies. These visual observations empirically suggest that two time scales govern the relaxation process, with the duration of *Stage II* related to the branch relaxation time and the duration of *Stage III* associated with the backbone relaxation time.

Molecular relaxation processes can be quantified by measuring the end-to-distance of the main chain backbone over time (Figure 3b). Here, we plot fractional backbone extension (x/L) by normalizing the instantaneous chain extension by the backbone contour length ($L_{30k,stained} = 13.6$ μm). Interestingly, single molecule trajectories clearly show that relaxation processes are dependent on molecular topology. In particular, we observe slower chain relaxation for branched polymers (1, 2, or 3 side branches) compared to a linear reference polymer with identical backbone molecular weight. We quantify this relaxation process to further probe chain topology effects. The longest relaxation time (*Stage III*) is dominated by the slowest mode at relatively small fractional extensions (e.g., $x/L < 0.30$). The longest relaxation time can be determined by fitting backbone relaxation data over this region to a Rouse-inspired single exponential decay: $(x/L)^2 = c_1 \exp(-t/\tau) + c_2$, where τ is the longest relaxation time of the linear polymer and c_1 and c_2 are fitting constants.[33,37,38] Due to the separation of time scales observed in Figure 3a for the branch (10 kbp) and backbone (30 kbp) motions, we interpret this long-time relaxation as that of the backbone experiencing extra frictional drag due to fully relaxed side branches. Based on this reasoning, we can determine the longest relaxation time of the comb polymer backbone using a single exponential fit between fractional extensions $0.14 < x/L < 0.30$, such that the

DOI: 10.1021/acsmacrolett.5b00140
ACS Macro Lett. 2015, 4, 446−452

low end of this range corresponds to distances over which backbone stretch can be accurately tracked using diffraction-limited fluorescence imaging. Using this approach, we determine longest relaxation times for linear polymers ($\tau_{linear,III}$ = 8.0 ± 0.9 s) and branched polymers with 1, 2, and 3 branches as $\tau_{1,III}$ = 8.0 ± 0.9 s, $\tau_{2,III}$ = 9.6 ± 1.1 s, and $\tau_{3,III}$ = 13.0 ± 1.7 s, respectively (Supporting Information, Figure S6). We note that no other time constants emerge when the same data are fit to a multiexponential decay, which further supports a single exponential decay function (Figure 3b, inset).

Comb polymer molecules with three side branches exhibit a significant increase in the longest relaxation time. However, the impact of one or two branches appears to be negligible in the context of the longest relaxation time, at least for this particular set of branch (10 kbp) and backbone (30 kbp) molecular weights. In order to further probe this effect, we also considered the intermediate relaxation time scale (*Stage II*). Based on multimode models for polymer dynamics in dilute solutions (e.g., Rouse model),[37,38] we considered the possibility of multiple modes (i.e., multiple relaxation time scales) by fitting the relaxation data in the intermediate extension region ($0.30 < x/L < 0.50$) to a multiexponential function. However, we found that these data were best fit to a single exponential decay with only a single time constant, which reveals a strong dependence of the relaxation time on the number of branches: $\tau_{linear,II}$ = 4.7 ± 0.6 s, $\tau_{1,II}$ = 4.2 ± 0.6 s, $\tau_{2,II}$ = 5.7 ± 0.8 s, and $\tau_{3,II}$ = 7.0 ± 1.0 s. Clearly, over these time scales, the presence of two or three branches slows intermediate relaxation processes.

In addition to branch grafting densities, our data also show that the position of the branch point along the main chain backbone has a direct impact on polymer relaxation. In Figure 3c, we consider several relaxation trajectories for molecules with a single branch located at different positions. Each curve indicates an ensemble of singly branched molecules wherein branch position is classified relative to the surface-tethered point (e.g., branch point at first third of backbone near tether, middle third, and last third near the free end). Intermediate relaxation times reflect a strong dependence on branch position, such that we observe slower relaxation when a branch exists farther from the surface tether: τ_{tether} = 2.5 ± 0.5 s, τ_{mid} = 4.7 ± 0.5 s, and τ_{end} = 5.6 ± 1.0 s. Interestingly, polymers with 1 branch near the tether point appear to relax faster than the linear backbone counterparts ($\tau_{linear,II}$ = 4.8 ± 0.6 s). However, the longest relaxation times of these molecular ensembles show no significant differences compared to the linear reference polymer.

From these data, we consider two related effects on the (*Stage II*) relaxation of the branch as it pertains to the backbone relaxation probed by the flow cessation experiments. First, we hypothesize the existence of a new relaxation mode spanning from the tether point to the end of the branch. When the branch point is positioned near the end of the polymer backbone, then this mode is likely more dominant than the primary mode along the main chain backbone. In this case, the relaxation of the comb polymer backbone is slower than that of a linear chain. Second, we hypothesize the importance of hydrodynamic flow fields induced by branch relaxations. When the branch point is positioned near the tether point, the aforementioned branch-based relaxation mode induces a local fluid flow more strongly than the slowly relaxing backbone. We postulate that the branch hydrodynamically drives the relaxation of the main chain near the tether point, which can result in a more rapid relaxation of the comb polymer backbone than that of a linear chain. More elaborate branch-wall hydrodynamic coupling could be possible, similar to effects important for linear chains near surfaces.[39−41] From a broader perspective, it is important to note that these branch effects can only be observed using single molecule experiments that can resolve branch position along a polymer chain backbone.

In summary, we report the synthesis and direct observation of topology-controlled relaxation dynamics of branched DNA polymers. Using this approach, our work extends single polymer investigations to a new class of polymers with nonlinear branched topologies. In particular, our data reveal the influence of branch grafting distributions on polymer relaxation dynamics. We observe that the relaxation of a surface-tethered polymer with 1 branch depends strongly on branch position; we also observe that surface-tethered polymers with at least two branches relax more slowly than linear polymers. Our results motivate intriguing questions for further study, including an investigation of the relaxation modes within a branched polymer and the dynamic stretching behavior of single branched polymers in free-solution flows. From a broader perspective, the versatility of PCR combined with non-natural nucleotides and SPAAC enables an extensive design space for branched polymer synthesis. For example, long-range PCR can readily yield chemically modified branch and backbone molecules approaching 50 kbp.[42] The application of SMFM to this design space enables in-depth studies of single molecule dynamics of branched polymers. Future experimental work with these polymers, including direct visualization of polymer chain dynamics in flow (tethered shear, simple shear, or planar extensional flow) and at varying concentrations (dilute or semidilute in linear, circular, or branched polymer backgrounds), will enable a fundamental molecular-based understanding of the nonequilibrium dynamics of branched polymers.

■ ASSOCIATED CONTENT

Supporting Information

Details of polymer synthesis, flow cell fabrication, surface preparation, single molecule imaging, end-to-end length distributions, branch frequency distributions, and relaxation experiments are provided. This material is available free of charge via the Internet at http://pubs.acs.org.

■ AUTHOR INFORMATION

Corresponding Author

*E-mail: cms@illinois.edu.

Notes

The authors declare no competing financial interest.

■ ACKNOWLEDGMENTS

This work was funded by an Illinois Distinguished Fellowship and an NSF Graduate Research Fellowship for DJM; the David and Lucile Packard Foundation, NSF CAREER Award CBET-1254340, and the Camille and Henry Dreyfus Foundation for CMS. The authors acknowledge the Roy J. Carver Biotechnology Center for gel imaging facilities and thank Sarah Kuhl for assistance with data processing.

■ REFERENCES

(1) Dealy, J. M.; Larson, R. G. *Structure and Rheology of Molten Polymers*; Hanser Publications: Cincinnati, OH, 2006.
(2) Zimm, B. H.; Kilb, R. W. *J. Polym. Sci.* **1959**, *37*, 19.

DOI: 10.1021/acsmacrolett.5b00140
ACS Macro Lett. 2015, 4, 446−452

(3) Larson, R. G. *The Structure and Rheology of Complex Fluids*; Oxford University Press: New York, 1998.
(4) Bovey, F. A.; Schilling, F.; McCrackin, F.; Wagner, H. L. *Macromolecules* **1976**, *9*, 76.
(5) Voit, B. I.; Lederer, A. *Chem. Rev.* **2009**, *109*, 5924.
(6) Snijkers, F.; Ratkanthwar, K.; Vlassopoulos, D.; Hadjichristidis, N. *Macromolecules* **2013**, *46*, 5702.
(7) van Ruymbeke, E.; Lee, H.; Chang, T.; Nikopoulou, A.; Hadjichristidis, N.; Snijkers, F.; Vlassopoulos, D. *Soft Matter* **2014**, *10*, 4762.
(8) Lentzakis, H.; Vlassopoulos, D.; Read, D.; Lee, H.; Chang, T.; Driva, P.; Hadjichristidis, N. *J. Rheol.* **2013**, *57*, 605.
(9) Larson, R. G. *Science* **2011**, *333*, 1834.
(10) Chen, B.; van der Poll, D. G.; Jerger, K.; Floyd, W. C.; Fréchet, J. M. J.; Szoka, F. C. *Bioconjugate Chem.* **2011**, *22*, 617.
(11) Chen, B.; Jerger, K.; Fréchet, J. M. J.; Szoka, F. C., Jr *J. Controlled Release* **2009**, *140*, 203.
(12) Chen, Y.; Thorn, M.; Christensen, S.; Versek, C.; Poe, A.; Hayward, R. C.; Tuominen, M. T. *Nat. Chem.* **2010**, *2*, 503.
(13) de Vos, W. M.; Leermakers, F. A. M.; Lindhoud, S.; Prescott, S. W. *Macromolecules* **2011**, *44*, 2334.
(14) Chambon, P.; Fernyhough, C. M.; Im, K.; Chang, T.; Das, C.; Embery, J.; McLeish, T. C. B.; Read, D. J. *Macromolecules* **2008**, *41*, 5869.
(15) Kapnistos, M.; Vlassopoulos, D.; Roovers, J.; Leal, L. G. *Macromolecules* **2005**, *38*, 7852.
(16) Daniels, D. R.; McLeish, T. C. B.; Crosby, B. J.; Young, R. N.; Fernyhough, C. M. *Macromolecules* **2001**, *34*, 7025.
(17) Kapnistos, M.; Kirkwood, K. M.; Ramirez, J.; Vlassopoulos, D.; Leal, L. G. *J. Rheol.* **2009**, *53*, 1133.
(18) Snijkers, F.; Van Ruymbeke, E.; Kim, P.; Lee, H.; Nikopoulou, A.; Chang, T.; Hadjichristidis, N.; Pathak, J.; Vlassopoulos, D. *Macromolecules* **2011**, *44*, 8631.
(19) McLeish, T. C. B. *Adv. Phys.* **2002**, *51*, 1379.
(20) McLeish, T. C. B.; Larson, R. G. *J. Rheol.* **1998**, *42*, 81.
(21) Lentzakis, H.; Das, C.; Vlassopoulos, D.; Read, D. J. *J. Rheol.* **2014**, *58*, 1855.
(22) Mai, D. J.; Brockman, C.; Schroeder, C. M. *Soft Matter* **2012**, *8*, 10560.
(23) Marciel, A. B.; Schroeder, C. M. *J. Polym. Sci., Part B: Polym. Phys.* **2013**, *51*, 556.
(24) Shaqfeh, E. S. G. *J. Non-Newtonian Fluid Mech.* **2005**, *130*, 1.
(25) Latinwo, F.; Schroeder, C. M. *Soft Matter* **2011**, *7*, 7907.
(26) Brockman, C.; Kim, S. J.; Schroeder, C. M. *Soft Matter* **2011**, *7*, 8005.
(27) Perkins, T. T.; Smith, D. E.; Chu, S. *Science* **1997**, *276*, 2016.
(28) Schroeder, C. M.; Babcock, H. P.; Shaqfeh, E. S.; Chu, S. *Science* **2003**, *301*, 1515.
(29) Heuer, D. M.; Saha, S.; Archer, L. A. *Electrophoresis* **2003**, *24*, 3314.
(30) Saha, S.; Heuer, D. M.; Archer, L. A. *Electrophoresis* **2006**, *27*, 3181.
(31) Sean, D.; Slater, G. W. *Electrophoresis* **2013**, *34*, 745.
(32) Selvin, P. R.; Ha, T. *Single-Molecule Techniques: A Laboratory Manual*; Cold Spring Harbor Laboratory Press: Cold Spring Harbor, NY, 2008.
(33) Ladoux, B.; Doyle, P. S. *Europhys. Lett.* **2000**, *52*, 511.
(34) Augustin, M. A.; Ankenbauer, W.; Angerer, B. *J. Biotechnol.* **2001**, *86*, 289.
(35) Zhu, Z.; Waggoner, A. S. *Cytometry* **1997**, *28*, 206.
(36) Ramsay, N.; Jemth, A.-S.; Brown, A.; Crampton, N.; Dear, P.; Holliger, P. *J. Am. Chem. Soc.* **2010**, *132*, 5096.
(37) Doi, M.; Edwards, S. F. *The Theory of Polymer Dynamics*; Clarendon Press, Oxford University Press: Oxford; Oxfordshire; New York, 1986.
(38) Rouse, P. E. *J. Chem. Phys.* **1953**, *21*, 1272.
(39) Brenner, H. *Chem. Eng. Sci.* **1961**, *16*, 242.
(40) Ma, H. B.; Graham, M. D. *Phys. Fluids* 2005, *17*.
(41) Sing, C. E.; Alexander-Katz, A. *Macromolecules* **2011**, *44*, 9020.
(42) Fuller, D. N.; Gemmen, G. J.; Rickgauer, J. P.; Dupont, A.; Millin, R.; Recouvreux, P.; Smith, D. E. *Nucleic Acids Res.* **2006**, *34*, e15.

DOI: 10.1021/acsmacrolett.5b00140
ACS Macro Lett. 2015, 4, 446−452